THE JOURNAL OF BIOLOGICAL CHEMISTRY VOL. 282, NO. 28, pp. 20553–20560, July 13, 2007

Heat Shock Protein 75 (TRAP1) Antagonizes Reactive Oxygen Species Generation and Protects Cells from Granzyme M-mediated Apoptosis*

Received for publication, April 16, 2007, and in revised form, May 18, 2007 Published, JBC Papers in Press, May 18, 2007, DOI 10.1074/jbc.M703196200

Guoqiang Hua, Qixiang Zhang, and Zusen Fan[1]

From the National Laboratory of Biomacromolecules and Center for Infection and Immunity, Institute of Biophysics, Chinese Academy of Sciences, Beijing 100101, China

Natural killer (NK) cells play an important role in innate immunity against virally infected or transformed cells as the first defense line. Granzyme M (GzmM) is an orphan granzyme that is constitutively highly expressed in NK cells and is consistent with NK cell-mediated cytolysis. We recently demonstrated that GzmM induces caspase-dependent apoptosis with DNA fragmentation through direct cleavage of inhibitor of caspase-activated DNase (ICAD). However, the molecular mechanisms for GzmM-induced apoptosis are unclear. We found GzmM causes mitochondrial swelling and loss of mitochondrial transmembrane potential. Moreover, GzmM initiates reactive oxygen species (ROS) generation and cytochrome *c* release. Heat shock protein 75 (HSP75, also known as TRAP1) acts as an antagonist of ROS and protects cells from GzmM-mediated apoptosis. GzmM cleaves TRAP1 and abolishes its antagonistic function to ROS, resulting in ROS accumulation. Silencing TRAP1 through RNA interference increases ROS accumulation, whereas TRAP1 overexpression attenuates ROS production. ROS accumulation is in accordance with the release of cytochrome *c* from mitochondria and enhances GzmM-mediated apoptosis.

Cytotoxic T lymphocytes (CTLs)[2] and natural killer (NK) cells are effector lymphocytes that are necessary for defense against virus-infected or transformed cells (1, 2). These cytolytic lymphocytes use the granule exocytosis pathway, which release perforin (PFP) and granzymes (Gzms) from cytolytic granules into an immunological synapse formed with their target (3). GzmA and B are the most abundant Gzms in mice and humans and have been most extensively studied (4–8). However, less is known about how other Gzms work in granule-mediated apoptosis. These Gzms are called orphan Gzms, which are also highly conserved serine proteases found in both humans and rodents, located in three clusters on separate chromosomes. The orphan Gzms include C, D, E, F, G, K, L, M, and N in mice, and H, K, and M in humans (9). GzmM is an orphan Gzm that cleaves preferentially after methionine, leucine, or norleucine (10). GzmM is constitutively highly expressed in NK cells, whereas it is not expressed in $CD4^+$ or $CD8^+$ T cells either constitutively or after stimulation (11). Kelly *et al.* (12) reported that GzmM induces a novel form of perforin-dependent death without caspase activation and DNA fragmentation. However, we recently demonstrated that GzmM induces caspase-dependent apoptosis with DNA fragmentation through direct cleavage of ICAD (13). Moreover, GzmM degrades the DNA damage sensor enzyme PARP to prevent cellular DNA repair and force apoptosis.

Reactive oxygen species (ROS) are potent inducers of oxidative damage and have been proposed as critical regulators of apoptosis (14). ROS can induce opening of the permeability transition (PT) pore through oxidation-dependent mechanisms and are potent inducers of apoptosis, both in cultured cells and *in vivo* (14). Notably, intracellular ROS arise prior to cytochrome *c* (cyt c) release during the activation of several apoptosis pathways. Mitochondrial damage is a required initial step in caspase-dependent apoptosis, including that induced by GzmB, in which it is triggered by proteolytic cleavage of Bid (15–17). GzmB and GzmC can also induce mitochondrial damage independently of the caspases (18–20). Lieberman and coworkers (21) recently reported that GzmA induces a rapid increase of ROS and mitochondrial transmembrane potential loss, but does not cleave Bid or cause apoptogenic factor release. Kelly *et al.* (12) reported GzmM changed the morphology of mitochondria to be rounded but not to be dilated. However GzmM does not alter the mitochondrial transmembrane potential ($\Delta\Psi$) or does not cause ROS accumulation and release of cyt c. It is unclear whether mitochondria are involved in GzmM-mediated apoptosis.

Tumor necrosis factor receptor-associated protein 1 (TRAP1) was initially identified using the yeast two-hybrid system as a novel protein that interacts with the intracellular domain of type I TNF receptor (22). TRAP1 is identical to heat shock protein 75 (HSP75), which is a member of the HSP90 family that binds to the retinoblastoma protein during mitosis and after heat shock (23). TRAP1 localizes in mitochondria and

* The work was supported by the National Natural Science Foundation of China Program 30470365 (to Z. F.) and the Outstanding Youth Grant (to Z. F.) (30525005), Grants from the 973 Programs (2006CB504303; 2006CB910901), The Hundred Talents Program, and the Knowledge Innovation Program of CAS (KSCX2-YW-R-42) (to Z. F.). The costs of publication of this article were defrayed in part by the payment of page charges. This article must therefore be hereby marked "*advertisement*" in accordance with 18 U.S.C. Section 1734 solely to indicate this fact.

[1] To whom correspondence should be addressed: National Laboratory of Biomacromolecules and Center for Infection and Immunity, Inst. of Biophysics, Chinese Academy of Sciences, 15 Datun Rd., Beijing 100101, China. Tel.: 010-64888457; Fax: 010-64871293; E-mail: fanz@moon.ibp.ac.cn.

[2] The abbreviations used are: CTL, cytotoxic T lymphocytes; Gzm, granzyme; PFP, pore-forming protein; Ad, adenovirus; NK cell, natural killer cell; TRAP1, tumor necrosis factor receptor-associated protein 1; ROS, reactive oxygen species; DMEM, Dulbecco's modified Eagle's medium; FACS, fluorescent-activated cell sorter; HA, hemagglutinin.

its mitochondrial localization sequence exists at the N terminus of this protein (24). A recent report showed TRAP1 is dramatically suppressed in tumor cells with apoptogenic inducers, such as the shikonin derivative β-hydroxyisovalerylshikonin (β-HIVS) or a topoisomerase II inhibitor VP16. TRAP1 silencing enhances cyt c release and apoptosis induced by those two apoptotic inducers (25). Im *et al.* (26) showed TRAP1-overexpressing cells decrease ROS generation after treatment of the deferoxamine. These data suggest TRAP1 may play an important role in antagonizing apoptosis via reducing ROS accumulation. In this study, we demonstrated GzmM can cause mitochondrial swelling and loss of ΔΨ. Furthermore, GzmM induces a rapid increase of intracellular ROS and the release of cyt c. TRAP1 is able to protect cells from death through inhibition of ROS generation. GzmM directly cleaves TRAP1 resulting in intracellular ROS accumulation. Moreover cells with silenced TRAP1 expression are more susceptible, whereas cells overexpressing TRAP1 are more resistant to GzmM-induced apoptosis.

MATERIALS AND METHODS

Cell Lines, Antibodies, and Reagents—Cells were grown in RPMI 1640 (Jurkat) or DMEM medium (HeLa) supplemented with 10% fetal calf serum, 50 μM β-mercaptoethanol, 100 units/ml penicillin, and streptomycin. Commercial antibodies were mouse mAb against cytochrome *c* (BD Pharmingen), β-actin, horseradish peroxidase-conjugated sheep anti-mouse IgG (Santa Cruz) and Alexa488-conjugated donkey anti-mouse IgG (Molecular Probes). A monoclonal antibody against human TRAP1(TRAP1–6) was kindly provided by Drs. D. O. Toft and S. J. Felts (Mayo Graduate School, Rochester, MN) or obtained from Abcam Ltd (Cambridge, UK). The fluorescent probe, 2′,7′-dichlorofluorescin diacetate (DCF-DA) was from Molecular Probes. 4,5-Dihydroxyl-1,3-benzene-disulfonic acid (Tiron) and cyclosporine A (CsA) were from Sigma. LipofectamineTM2000 was from Invitrogen. Annexin V-FITC was from BD Pharmingen, ProLong Antifade kit was from Molecular Probes.

Recombinant Protein Expression—Recombinant GzmM, S-AGzmM (enzymatically inactive GzmM produced by mutating the active site Ser^{182} to Ala) were produced and purified as previously described (13). Full-length cDNA coding human TRAP1 (a gift from S. J. Felts) was subcloned into pET26b(+) and expressed in *Escherichia coli* strain BL21(DE3). Recombinant TRAP1 with His_6 tags were purified through a nickel column as above.

Loading GzmM with Adenovirus—Cells were washed three times in HBSS and resuspended in loading buffer (HBSS with 0.5 mg of bovine serum albumin per ml, 1 mM $CaCl_2$, 1 mM $MgCl_2$). HeLa cells or Jurkat cell (2×10^5) in 50 μl of loading buffer were incubated at 37 °C for the indicated times with different concentrations of GzmM, S-AGzmM, and an optimal dose of adenovirus (Ad). Cells were incubated for an additional 15 min in 1 mM phenylmethylsulfonyl fluoride before being lysed for immunoblot.

Transmission Electron Microscopy—HeLa cells (5×10^5) were treated with GzmM plus Ad at 37 °C for 4 h. Then cells were washed twice and fixed with 2% glutaraldehyde at 4 °C for 1 h and postfixed with 2% osmium tetroxide. Cells were dehydrated with sequential immerge in 50, 70, 80, 90, and 100% ethanol, and then embedded in Spurrs resin. Ultrathin sections were mounted in copper grids and counterstained with uranyl acetate and lead citrate. Images were photographed and scanned by Eversmart Jazz+ program (Scitex).

Assessment of ΔΨ—For ΔΨ, cells treated with GzmM/Ad or CCCP were stained with $DiOC_6$ (3) and analyzed by flow cytometry as described (27). In brief, Jurkat cells treated with GzmM/Ad (100pfu/ml) for the indicated times and doses were harvested and washed with HBSS three times. Cells were loaded with 20 nM 3,3′-dihexyloxacarbocyanine iodide $DiOC_6$ (3) for 5 min before FACS analysis. Cells treated with the membrane uncoupler carbonyl cyanide *m*-chlorophenylhydrazone (CCCP) were used as a positive control.

Cleavage Assay—Cell lysates prepared from HeLa cells treated with Nonidet P-40 lysis buffer (0.5% Nonidet P-40/25 mM KCl/5 mM $MgCl_2$/1 mM phenylmethylsulfonyl fluoride/10 mM Tris-HCl, pH 7.6). Cell lysates (equivalent to 2×10^5 cells) or 1 μM rTRAP was incubated with indicated doses of GzmM or S-AGzmM for the indicated time points in 20 μl of cleavage buffer (50 mM Tris-HCl pH 7.5, 1 mM $CaCl_2$, 1 mM $MgCl_2$). For *in vivo* cleavage assay, cells loaded with GzmM/Ad were lysed in 0.5% Nonidet P-40 lysis buffer. The reaction samples were terminated in 5× SDS-loading buffer and probed by immunoblotting.

ATPase Activity Assay—ATP hydrolysis was measured directly by the conversion of ATP to ADP, release of inorganic phosphate (P_i) was estimated according to Kempaiah and Srinivasan (28). Briefly, TRAP1 (3 μM) was incubated with 1 mM ATP at 37 °C for indicated times in 100 μl of buffer containing 10 mM Hepes-KOH, pH 7.4, and 5 mM $MgCl_2$, 120 mM KCl. Inhibition by granzyme M was performed with 3 μM TRAP1, 1 mM ATP, and various amounts of granzyme M. Reactions were stopped by addition of 200 μl of 1% SDS. Following treatment, samples (0.1 ml) were added to 0.7 ml of ascorbate-molybdate reagent, which consists of 1 part of 10% ascorbic and 6 parts of 0.42% (w/v) ammonium molybdate in 1 N H_2SO_4. Tubes were incubated at 45 °C for 20 min, and absorbance was determined at 820 nm.

Time-lapse Microscopy—HeLa cells were plated overnight in 35-mm culture dishes in DMEM and replaced with phenol red-free DMEM with 2′,7′-dichlorofluorescin diacetate (DCF-DA), followed by treatment with GzmM (1 μM) and Ad. Images were taken every 2 min by Olympus IX71 microscope (29).

Measurement of Intracellular ROS—Intracellular ROS production was monitored by incubating HeLa cells with 10 μM DCF-DA at 37 °C for 30 min. Unincorporated DCF-DA was removed through complete washing with phosphate-buffered saline before loading GzmM with Ad. Fluorescence was measured using a flow cytometer (FACSCalibur). 200 μM H_2O_2-treated cells were as a positive control.

Apoptosis and Cytochrome c Release Assay—Phosphatidylserine externalization was stained with Annexin V-fluorescein isothiocyante labeling and assessed with flow cytometer. For the analysis of cyt c release, HeLa cells (1×10^6) were treated with GzmM plus Ad at the indicated times. Cells were washed twice with PBS and resuspended in 100 μl of digitonin lysis

buffer (80 mM KCl, 250 mM sucrose, 0.02% digitonin) for 5 min (18). The supernatants and the pellets were resolved on 15% SDS-PAGE and detected by immunoblotting using cyt c antibody.

Laser Scanning Confocal Microscopy—HeLa cells were grown overnight to subconfluency at 37 °C in 8-well chamber slides coated with rat collagen I (BD Falcon™) and incubated with 500 nM MitoTracker (Molecular Probes) for 30 min according to the manufacturer's instruction. Cells were treated with 1 μM GzmM in the presence or absence of Ad for 4 h, washed, and fixed with 4% paraformaldehyde for 20 min at room temperature and permeabilized with 0.1% Triton X-100 for another 20 min, the cells were incubated at room temperature for 1 h with 5 μg/ml anti-cyt c mAb (clone 6H2.B4; Pharmingen), 50 μg/ml donkey serum and 100 μg/ml RNase I. The cells were stained with Alexa 488-conjugated donkey anti-mouse IgG, and soaked for 5 min in phosphate-buffered saline containing 0.1 μg/ml Hoechst. The slides were mounted with ProLong Antifade reagent and observed using laser scanning confocal microscopy (Olympus FV500 microscope).

Silencing and Overexpression of TRAP1—Three pairs of RNA sequences against TRAP1 for RNAi were designed based on pSUPER system instructions (Oligoengine) and cloned into pSUPER-puro that expresses 19-nt hairpin-type short hairpin RNAs (shRNAs) with a 9-nt loop, as described previously (30). TRAP1 shRNA-encoding sequences were as follows: shRNA1: 5′-ACATGAGTTCCAGGCCGAGTTCA-AGAGACTCGGCCTGGAACTCATGTTTTTTT-3′ (sense) and 5′-AAAAAAACATG AGTTCCAGGCCGAGTCTCTT-GAACTCGGCCTGGAACTCATGT-3′ (antisense); shRNA2: 5′-GTACAGCAACTTCGTCAGCTTCAAGAGAGCTGACG-AAGTTGCTGTACTTTTTT-3′(sense) and 5′-AAAAAAGT-ACAGCAACTTCGTCA GCTCTCTTGAAGCTGACGAAG-TTGCTGTAC-3′ (antisense); shRNA3: 5′-ACATGAGTTCC-AGGCCGAGTTCAAGAGACTCGGCCTGGAACTCATGT-TTTTTT-3′ (sense) and 5′-AAAAAAA CATGAGT TCCA-GGCCGAGTCTCTTGAACTCGGCCTGGAACTCATGT-3′ (antisense). The inserted shRNAs were confirmed by DNA sequencing. HeLa cells were transfected by using Lipofectamine 2000 (Invitrogen) as described by the manufacturer. Cells with silenced TRAP1 were selected with puromycin. Empty vectors were used as a control. For TRAP1 overexpression, HeLa cells were transfected with either empty vector pCMV-HA or pCMV-HA-TRAP1 for 3 days.

RESULTS

GzmM Targets Mitochondria and Causes Loss of ΔΨ—We previously demonstrated GzmM induces caspase-dependent apoptosis (13). Kelly *et al.* (12) reported GzmM induces caspase-independent cell death, which changed the morphology of mitochondria to be rounded but not to be dilated. We wanted to verify whether mitochondria are involved in GzmM-mediated apoptosis. To investigate whether GzmM provokes morphological changes of mitochondria, 1 μM GzmM was loaded with Ad into HeLa cells at 37 °C for 4 h and visualized by electron microscopy. GzmM plus Ad treatment induced profound mitochondrial swelling with loss of cristae structures (Fig. 1). The mitochondria of mock-treated cells showed normal features with a condensed state and narrow cristae. The mitochondria of cells treated with S-AGzmM plus Ad or GzmM alone had no effect (Fig. 1 and not shown). Similar results were obtained by loading GzmM with PFP (data not shown).

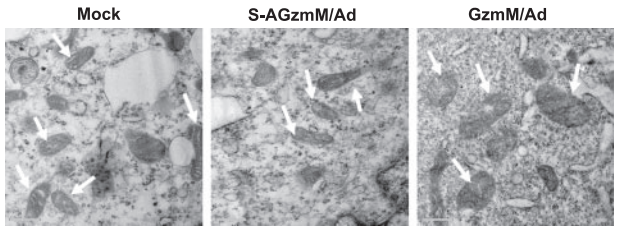

FIGURE 1. **GzmM causes mitochondrial swelling of target cells.** HeLa cells were incubated with 1 μM GzmM and Ad at 37 °C for 4 h and detected by a high-magnification transmission electron microscopy (×6500). The normal and inflated mitochondria are indicated with *arrows*.

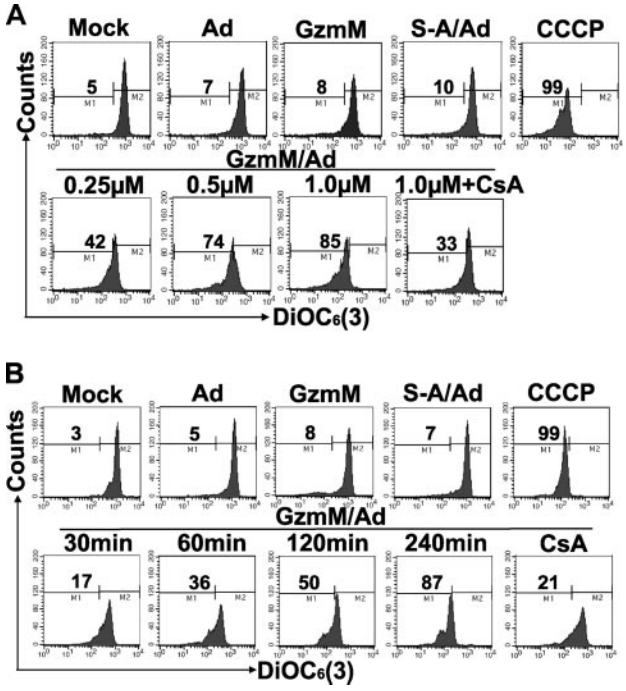

FIGURE 2. **GzmM initiates loss of ΔΨ.** Jurkat cells were treated for the indicated doses of GzmM or S-AGzmM(S-A) for 4 h in the presence of Ad (100 pfu/ml) at 37 °C (*A*) or the indicated times with 1 μM GzmM plus Ad (*B*). The classic uncoupler of oxidative phosphorylation CCCP (10 μM) was used as a positive control. Changes in ΔΨ were determined by 20 nM $DiOC_6$ (3). 20 μM CsA was used to treat cells prior to GzmM loading. These data are representative of at least three independent experiments.

Mitochondrial functions are dependent on the maintenance of ΔΨ (31). Loss of ΔΨ is likely to contribute to the death of cells (32). To assess whether GzmM causes ΔΨ collapse, Jurkat cells were treated with GzmM plus Ad and analyzed by FACS analysis. Cells loaded with GzmM plus Ad showed a dose-dependent decrease of ΔΨ, assayed by the change in fluorescence of the sensitive dye 3,3′-dihexyloxacarbocyanine iodide $DiOC_6$ (3) (Fig. 2*A*). 0.25 μM GzmM started to initiate significant reduction of ΔΨ. Inactive S-AGzmM plus Ad or mock-treated cells were without effect. An uncoupler of oxidative phosphorylation carbonyl cyanide *m*-chlorophenyl-hydrazone (CCCP) was used to treat cells as a positive control. GzmM-induced ΔΨ reduction was also in a time-dependent manner (Fig. 2*B*). 1 μM

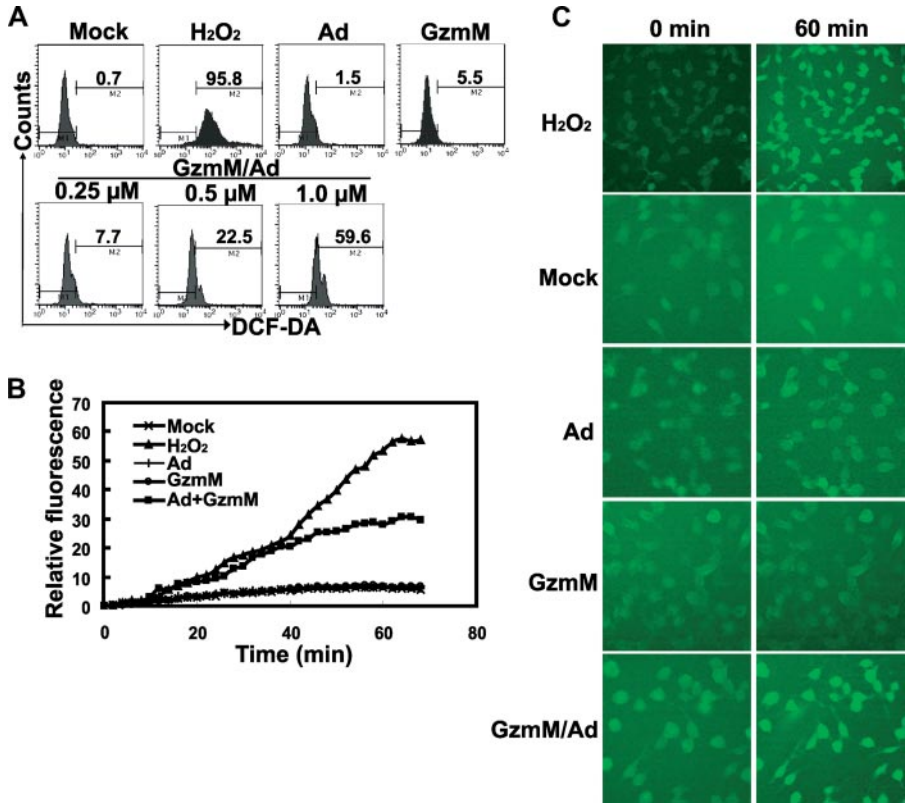

FIGURE 3. **GzmM induces a rapid increase of intracellular ROS.** *A*, GzmM loading of HeLa cells with Ad induces a dose-dependent increase of ROS. HeLa Cells pretreated with DCF-DA were loaded with different doses of GzmM in the presence of Ad for 1 h and analyzed by flow cytometry. H_2O_2 was used as a positive control. *B* and *C*, kinetics of GzmM-induced ROS production at a single cell level. HeLa cells stained with DCF-DA were treated with GzmM plus Ad, and followed by a time lapse fluorescence microscopy. The data are representative of three independent experiments.

GzmM plus Ad initiated a dramatic decrease in $\Delta\Psi$ within 1 h. By 4 h, $\Delta\Psi$ was completely collapsed. GzmM and Ad alone or S-AGzmM had little effect. PT pore can mediate mitochondrial swelling and depolarization during the course of apoptosis. We next investigated whether the PT pore inhibitor cyclosporine A (CsA) was capable of inhibiting the loss of $\Delta\Psi$ induced by GzmM. CsA significantly inhibited the loss of mitochondrial $\Delta\Psi$ induced by GzmM. These results indicate GzmM causes loss of $\Delta\Psi$ through disruption of the PT pore.

GzmM Induces a Rapid Increase of Intracellular ROS—ROS production has been identified as an early event undergoing apoptosis induced by a variety of stimuli. Superfluous ROS cause mitochondrial damage as well as nuclear DNA damage. Mitochondria are the major source of intracellular ROS (33). GzmA induces a rapid increase of ROS and mitochondrial transmembrane potential loss leading to caspase-independent death (21). We next wanted to determine whether ROS is accumulated during GzmM-mediated cytolysis. ROS production was detected using the dye DCF that is a nonfluorescent cell-permeant compound. Once entering a cell, it is degraded by endogenous esterases and no longer diffuses out of the cell. De-esterified products become the fluorescent compound 2′,7′-dichlorofluors upon oxidation by ROS. To detect ROS accumulation in GzmM-induced death, HeLa cells were treated with various amounts of GzmM plus Ad as measured by detection of the conversion of DCF to 2′,7′-dichlorofluorescin. 0.25 μM GzmM began to trigger ROS production within a 1-h treatment as measured by increase in mean fluorescence intensity (MFI) of the ROS indicator dye (Fig. 3*A*). GzmM augmented ROS generation with increasing concentrations. 1 μM GzmM reached a high peak for ROS production (MFI: 59.6). ROS accumulation required GzmM delivery by Ad. GzmM or Ad alone had no effect. Inactive mutant GzmM (S-AGzmM) plus Ad did not trigger ROS generation (not shown). H_2O_2-treated cells were used as a positive control. To further verify ROS generation induced by GzmM, time-lapse microscopy was used to visualize ROS production at a single cell level. HeLa cells were incubated in the presence of GzmM plus Ad, fluorescence staining dynamically condensed during induction of cell death (Fig. 3, *B* and *C*). GzmM and Ad alone treated cells were undetectable. One cell was chosen for detection of ROS generation by photographing every 2 min. ROS was produced early and increased over time, which was consistent with the above observations by FACS. H_2O_2 treated cells were used as a positive control. These data are representative of three separate experiments.

GzmM Directly Cleaves TRAP1—To investigate whether TRAP1 participates in GzmM-induced apoptosis, nanomolar concentrations of GzmM were incubated with recombinant TRAP1 (rTRAP1) at 37 °C for 2 h. GzmM began to degrade TRAP1 at a nanomolar concentration of 50 nM (Fig. 4 A). rTRAP1 began to degrade within 10 min with 0.5 μM GzmM treatment. Inactive S-AGzmM did not cause TRAP1 degradation. Neither caspase3 nor caspase 8 cut rTRAP1 (data not shown). We detected TRAP1 degradation in cytoplasmic lysates of HeLa cells. Native TRAP1 (2×10^5 cell equivalents) was almost cleaved at the dose of 1.0 μM GzmM at 37° for 2 h (Fig. 4*B*). GzmM began to degrade TRAP1 at a very early time of 10 min. The full-length of TRAP1 was completely degraded by 2 h. S-AGzmM was without effect on recombinant or native form of TRAP1. These data indicate TRAP1 cleavage requires enzymatic activity of GzmM.

To further verify TRAP1 processing is physiologically relevant, HeLa cells were treated with 1 μM GzmM in the presence of Ad. TRAP1 was cleaved in GzmM/Ad-loaded cells by 2 h (Fig. 4*C*). After 6 h, TRAP1 was completely cleaved. GzmM and Ad alone or S-AGzmM plus Ad failed to degrade TRAP1. The same blot was stripped and reprobed for β-actin. β-Actin was unchanged as a good loading control. The GzmM concentration required to cut TRAP1 *in vivo* is comparable to that required to induce cell death and DNA damage (13). Therefore, TRAP1 is a direct physiological substrate of GzmM *in vivo*.

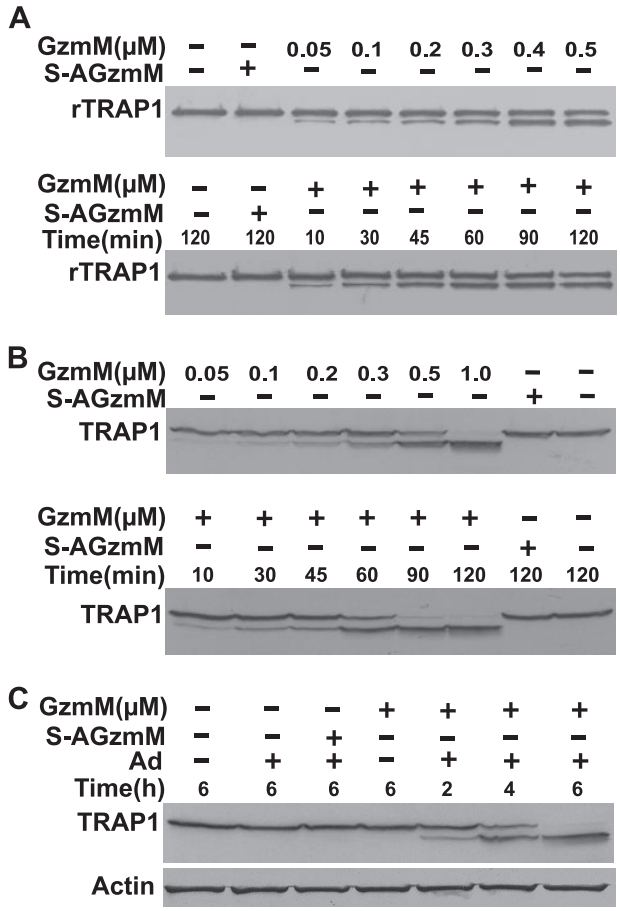

FIGURE 4. **TRAP1 is a physiological substrate of GzmM.** *A*, rTRAP1 was cleaved by GzmM in a dose- and time-dependent fashion. rTRAP1 (1 μM) was incubated with different concentrations of GzmM at 37 °C for 2 h or with 0.5 μM GzmM for the indicated times. The reactions were stopped by adding 5× SDS loading buffer and analyzed by immunoblotting with anti-TRAP1 Ab. *B*, GzmM cleaves native TRAP1. Cell lysates (2×10^5 Cell equivalents) were treated with different doses of GzmM at 37 °C for 2 h or with 1 μM GzmM for and time points. *C*, 2×10^5 HeLa cells were treated with 1.0 μM GzmM with Ad at 37 °C for the indicated times. The whole cell lysates were probed with anti-TRAP1 Ab. β-actin was unchanged as a negative control.

GzmM Disrupts the ATPase Activity of TRAP1—TRAP1 is an ATP-binding protein with ATPase activity (24). TRAP1 may play an important role in refolding of denatured proteins after oxidative stress. We next tested whether GzmM cleavage interferes with the ability of TRAP1 to hydrolyze ATP. ATPase assay was carried out to analyze the effect of GzmM on ATP hydrolysis by TRAP1. rTRAP1 possessed ATPase activity as shown in Fig. 5*A*. Incubation of rTRAP1 with ATP resulted in increasing free phosphates in a time-dependent manner. Preincubation of rTRAP1 with GzmM inhibited its ATPase activity in a dose-dependent manner (Fig. 5*B*). 2 μM GzmM can completely inhibit ATPase activity of TRAP1. Inactive S-AGzmM had no such effect.

Silencing TRAP1 Expression Enhances ROS Production Induced by GzmM—GzmM can induce a rapid increase of intracellular ROS as shown above. We next wanted to determine whether TRAP1 cleavage by GzmM contributes to trigger cell death through ROS accumulation. We designed three shRNA sequences against TRAP1 and constructed pSUPER-TRAP1-shRNA plasmids to silence TRAP1 expression that contained 19-nucleotide hairpin-type short hairpin RNAs.

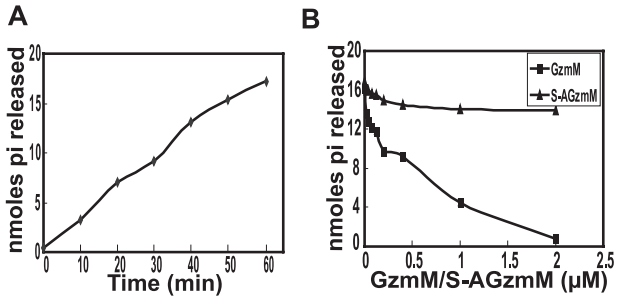

FIGURE 5. **The ATPase activity of TRAP1 is disrupted by GzmM.** *A*, time course of the catalysis of ATP hydrolysis. 3 μM rTRAP1 was incubated with 1 mM ATP and analyzed by using pi release assay over time. *B*, GzmM abolishes the ATPase activity of TRAP1. 3 μM rTRAP1 was pretreated with the indicated doses of GzmM for 1 h prior to adding 1 mM ATP. S-AGzmM was as a control. Each point represents the mean of three independent experiments.

These plasmids were separately transfected into HeLa cells. After 3 days, siRNA1 and siRNA2 each silenced TRAP1 expression by 60–70%; whereas siRNA3 had little effect on TRAP1 expression (Fig. 6*A*). pSUPER-TRAP1-shRNA1 stable cell lines were established by puromycin selection. TRAP1 was almost undetectable through immunoblotting. HeLa cells transfected with pSUPER empty vector were unchangable for expression of TRAP1.

With 50 μM H_2O_2 treatment, TRAP1 silenced HeLa cells got 34.6% ROS-positive. While only 11.9% control cells transfected with empty vector were ROS positive (Fig. 6*B*). Similar results were obtained with treatment of 100 μM H_2O_2. To further look at whether TRAP1 silencing enhances GzmM-induced ROS accumulation, TRAP1-silenced HeLa cells were loaded with GzmM plus Ad. ROS generation dramatically increased in TRAP1 silenced HeLa cells compared with cells transfected by empty vectors with increasing concentrations (0.25 μM: 28.9 *versus* 7.0%; 0.5 μM: 80.2 *versus* 31.2%; 1 μM: 98.9 *versus* 47.0%) (Fig. 6*C*). Cells treated with GzmM or Ad alone just got comparable levels of ROS. These results indicate that TRAP1 cleavage enhances ROS generation during GzmM-induced apoptosis.

TRAP1 Silencing Accelerates Cytochrome c Release and GzmM-induced Death—Cyt c release from mitochondria appears to be an early event during apoptosis induced by a variety of stimuli (35). Cytosolic cytochrome *c* together with Apaf-1 and procaspase-9 in a ATP-dependent manner forms apoptosome that causes caspase activation to orchestrate the biochemical execution of cells (36). Intracellular ROS arise prior to cyt c release during activation of several apoptotic pathways. GzmM can induce a rapid increase of intracellular ROS, we further detected whether GzmM induces cyt c release from mitochondria. Cyt c was released from mitochondria in HeLa cells treated with GzmM and Ad visualized through confocal microscopy (Fig. 7*A*). Cyt c was not released in response to treatment by Gzm M and Ad alone or S-AGzmM plus Ad (and data not shown).

We next wanted to test whether TRAP1 affects GzmM-induced cyt c release. HeLa cells with silenced TRAP1 were treated with GzmM plus Ad at 37 °C for different time points. Cyt c release occurred in HeLa cells with silenced TRAP1 at earlier time compared with those with transfection by empty vectors after treatment with GzmM and Ad (Fig. 7*B*). Cyt c was not detected in supernatants of control cells under identical

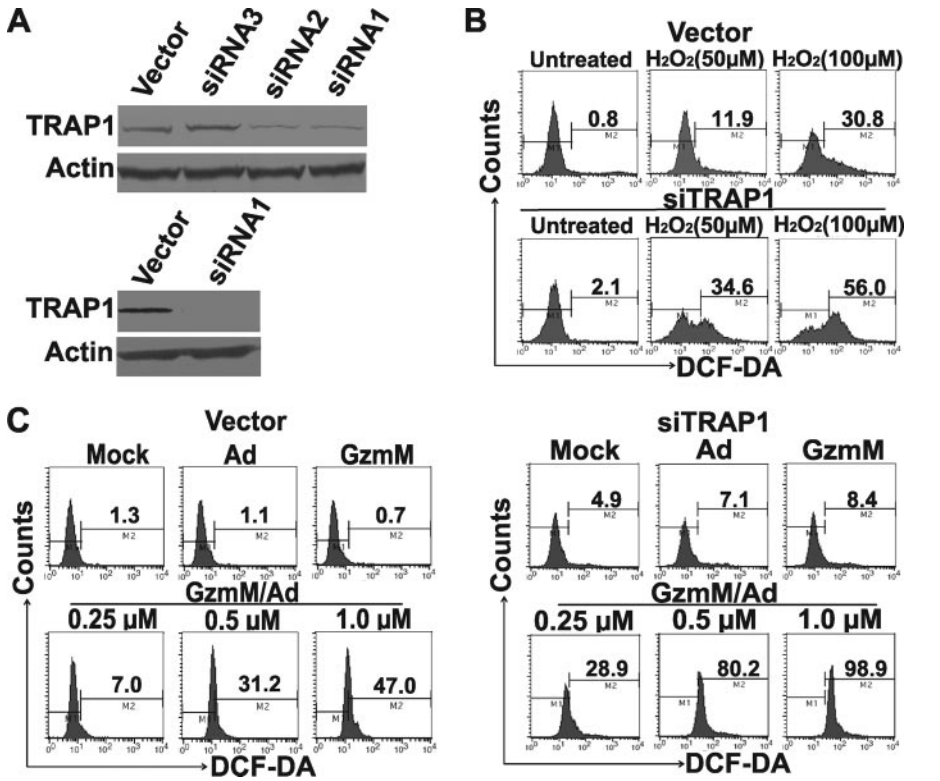

FIGURE 6. **Silencing TRAP1 expression enhances ROS production induced by GzmM.** *A*, TRAP1 was silenced by transfection with pSUPER-TRAP1-shRNA. Cells stably expressing TRAP1 siRNA were selected and TRAP1 was completely silenced. *B*, TRAP1 knockdown increases ROS accumulation exposed to H_2O_2. TRAP1 silenced HeLa cells were treated with the indicated doses of H_2O_2 and loaded with 10 μM DCF-DA, followed by FACS analysis. *C*, TRAP1 silencing enhances ROS generation. TRAP1 silenced HeLa cells were loaded with various amounts of GzmM plus Ad and analyzed as above. The results are representative of three separate experiments.

conditions until 3h. These data indicate TRAP1 silencing can accelerate cyt c release in GzmM-induced death.

We next verified whether TRAP1 can protect cells from GzmM-mediated cytolysis. Cells with silenced TRAP1 or empty vector control cells were treated with GzmM and Ad and assayed by Annexin V staining. Control cells obtained 40 ± 2% Annexin V positive. Annexin V positive rate in silenced TRAP1 cells increased (62 ± 3%) ($p < 0.02$) (Fig. 7*C*). To examine whether ROS is involved in GzmM-induced death, the cells were pretreated with the superoxide scavenger Tiron (50 mM) for 30 min, and treated with GzmM plus Ad. Tiron treatment can inhibit GzmM-induced death both in TRAP1 silenced or control cells (TRAP1 silencing: 19 ± 3% *versus* 62 ± 3%; control cells: 18 ± 2% *versus* 40 ± 2%).

Overexpression of TRAP1 Protects Cells from GzmM-induced Apoptosis through Attenuating ROS Generation—To further verify the role of TRAP1 in GzmM-induced

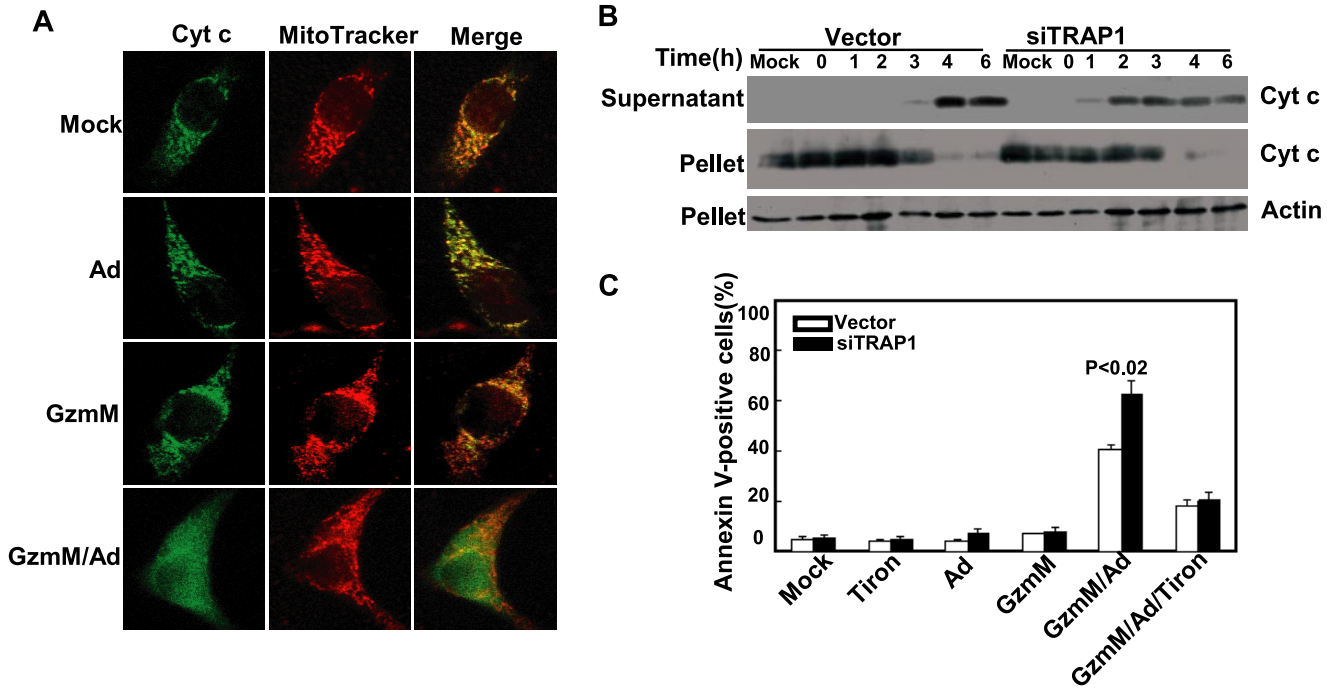

FIGURE 7. **TRAP1 silencing accelerates cytochrome *c* release and GzmM-induced apoptosis.** *A*, GzmM triggers cyt c release from mitochondria analyzed using confocol microscopy. HeLa cells were treated with 1 μM GzmM plus Ad at 37 °C for 4 h. Cyt c green fluorescence is shown at left, MitoTracker red in the middle, and the merged image at *right*. *B*, TRAP1 silenced HeLa cells with pSUPER-TRAP1-shRNA1 were treated with 1 μM GzmM and Ad for the indicated times, and the supernatants and the pellets were detected by immunoblotting using cyt c antibody. The results represent three independent experiments. *C*, TRAP1 silencing accelerates GzmM-induced apoptosis. TRAP1 silenced HeLa cells and control cells were treated with 1 μM GzmM plus Ad in the presence or absence of 50 mM Tiron. The extent of apoptosis was determined by staining with Annexin V-FITC. The results shown are means ± S.D.

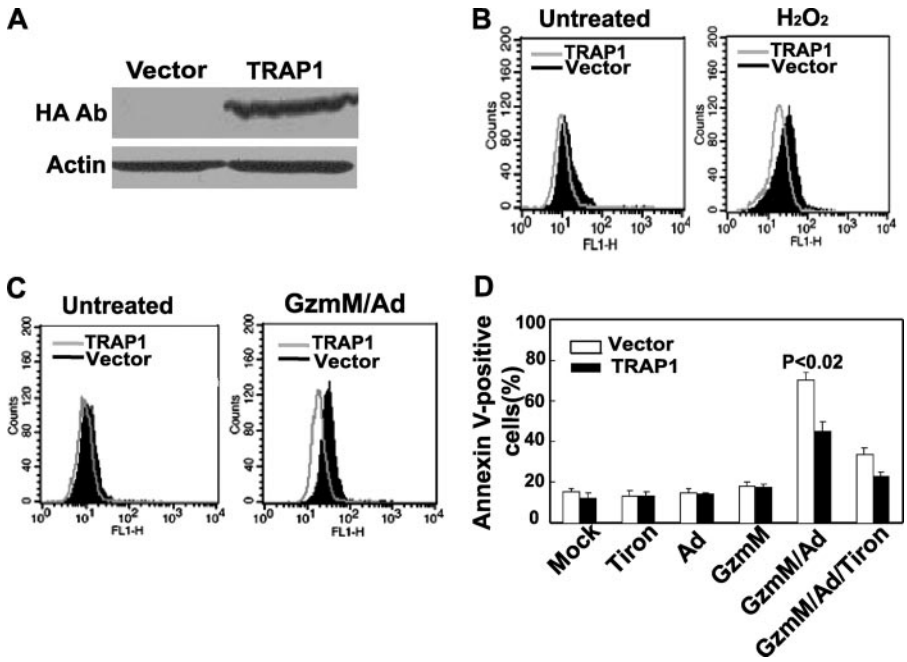

FIGURE 8. **Overexpression of TRAP1 inhibits GzmM-induced apoptosis through antagonizing ROS generation.** *A*, TRAP1 overexpression was obtained via transfection with pCMV-HA-TRAP1 for 3 days in HeLa cells. Cell lysates were analyzed by immunoblotting for anti-HA-tag. *B*, ROS decreases in TRAP1 overexpressed cells triggered by H_2O_2. *C*, TRAP1 antagonizes GzmM-induced ROS production. TRAP1 overexpressed HeLa cells were loaded with GzmM/Ad for 1 h. *D*, overexpression of TRAP1 inhibits GzmM-induced apoptosis. TRAP1-overexpressed HeLa cells and control cells were treated with 1 μM GzmM plus Ad in the presence or absence of 50 mM Tiron and then stained with Annexin V followed by flow cytometry. The data shown are mean ± S.D.

ROS generation, TRAP1 was overexpressed by transfection with pCMV-HA-TRAP1 in HeLa cells. 3 days later, the amount of TRAP1 in cells was detected by immunoblotting using HA tag antibody (Fig. 8*A*). pCMV-HA empty vector was transfected as a control. TRAP1 overexpression reduced the amount of endogenous ROS in HeLa cells after 100 μM H_2O_2 treatment (Fig. 8*B*). Similar results were obtained after treatment with 1 μM GzmM plus Ad (Fig. 8*C*). To further determine whether TRAP1 protects cells from GzmM-induced apoptosis, pCMV-HA-TRAP1 transfected cells were treated with 1 μM GzmM plus Ad. Overexpression of TRAP1 was less susceptible to GzmM-induced death compared with cells transfected with empty vectors assayed through Annexin V staining (45 ± 3% *versus* 69 ± 2%) (Fig. 8*D*) ($p < 0.02$). Tiron treatment can inhibit GzmM-induced death both in TRAP1 overexpressed or empty vector control cells (TRAP1 overexpression: 21 ± 2% *versus* 45 ± 3%; Control cells: 33 ± 3% *versus* 69 ± 2%). GzmM and Ad alone or Tiron itself caused comparable death.

DISCUSSION

GzmM is an orphan Gzm, highly expressed in NK cells but is not expressed in CD4+ or CD8+ T cells either constitutively or after stimulation. NK cells are the major effector cells of the innate immunity that act as the first line of defense against viral infection and tumors (37). Suck *et al.* (38) reported a human NK cell line KHYG-1 appears to have greater killing activity that is consistent with higher expression of GzmM, while GzmA and B are undetectable. It suggests GzmM might play an important role in NK cell-mediated cytolysis. Kelly *et al.* (12) reported GzmM causes a third major perforin-dependent death pathway besides GzmA and B. We recently demonstrated that GzmM induces typical apoptosis depending on caspase activation and CAD-mediated DNA fragmentation (13). However its molecular machinery of death is less defined. Here we demonstrate GzmM-induced apoptosis is dependent on mitochondrial damage. GzmM induces loss of $\Delta\Psi$ and a rapid accumulation of intracellular ROS. TRAP1 acts as an important ROS regulator to antagonize ROS generation. Cleavage of TRAP1 by GzmM might be central to ROS generation.

Mitochondria play an important role in the caspase-dependent death pathway, in which damage of the mitochondrial outer membrane (MOM) integrity releases a number of key intermembrane proteins, such as cyt c, SMAC, HtrA2, AIF, and EndoG that are released into the cytosol undergoing apoptosis (39). These events are initiated by the opening of the PT pore (5). Opening of the PT pore triggers an increase of inner membrane permeability to ions and solutes, followed by net water influx toward the mitochondrial matrix, swelling of the organelle, and physiological disruption of its outer membrane, with the consequent release of proteins to the intermembrane space. Increase of ROS and loss of $\Delta\Psi$ are indicative of mitochondrial dysfunction, hallmarks of apoptotic mitochondrial damage. It is postulated that ROS and $\Delta\Psi$ collapse are early events in apoptosis that are involved in the opening of the PT pore of the inner mitochondrial membrane. Kelly *et al.* (12) found GzmM induces caspase-independent cell death. GzmM triggered mitochondria to be rounded but not cause loss of $\Delta\Psi$ and other functions. However we found GzmM induces mitochondrial swelling and collapse of $\Delta\Psi$ through PT pore opening. GzmB and GzmC can induce mitochondrial damage independently of the caspases (18, 19). Lieberman group showed ROS is critical in GzmA-induced caspase-independent death. ROS generation induced by GzmA is not inhibited by Bcl-2 overexpression or by pan caspase inhibitors (21). Superoxide scavengers can block apoptosis by GzmA or CTLs expressing GzmA and/or GzmB. These findings indicate ROS is central to cytolysis induced by cytolytic lymphocytes.

Kelly *et al.* (12) still showed GzmM does not cause ROS accumulation and release of cyt c. We found GzmM triggers a rapid increase of intracellular ROS by targeting mitochondria and confirmed it at a single cell level. Both the antioxidant NAC and the superoxide scavenger Tiron blocked ROS production that protected cells from GzmM-induced death (data not shown). We identified that a key heat shock protein 75 (TRAP1) is a physiological substrate of GzmM that is localized in mitochon-

dria. Degradation of TRAP1 is responsible for accumulation of intracellular ROS induced by GzmM. TRAP1 (also know as HSP75) shows significant homology to members of the HSP90 family (24). TRAP1 also contains a pRb binding motif L*X*C*X*E (amino acids 470–474) through which it binds to pRb. Mutation of the L*X*C*X*E sequence to LXMXE blocks the TRAP1-pRb interaction. Like other heat shock proteins, TRAP1 can act as a chaperone to refold denatured pRb into its native conformation. The above functions are required for the cytoplasmic distribution of TRAP1. In this study, we found TRAP1 localizes in the mitochondria, which is consistent with the observation by Felts *et al.* (24). Cleavage by GzmM enhances a rapid increase of ROS. Cells with silenced TRAP1 expression are more prone to the generation of ROS, whereas cells overexpressing TRAP1 inhibit the production of ROS, which appears with similar dynamics to GzmM-induced cell death. We checked that other Gzms A, B, or K did not cleave TRAP1 (data not shown). Thus it suggests TRAP1 might be important to antagonize ROS accumulation in response to GzmM-mediated cell death.

ROS induce the opening of PT pore through oxidation-dependent mechanisms and are potent inducers of apoptosis (14). A cell is endowed with an extensive antioxidant defense system to combat ROS, either directly by interception or indirectly through reversal of oxidative damage. Once ROS overcome the defense systems of the cell, the redox homeostasis is altered, which leads to oxidative stress. HSPs are among the subset of oxidative stress-responsive proteins known to prevent protein aggregation. In addition, HSPs may directly regulate specific stress-responsive signaling pathways and may antagonize signaling cascades that result in apoptosis. HSP70 protects cells from a number of apoptotic stimuli, such as heat shock, radiation and oxidative stress. HSP90 appears to be involved in the inhibition of apoptosis by suppressing the cyt c-mediated oligomerization of Apaf-1 (34). HSP25 down-regulates PKCδ that is a key molecule for radiation-induced ROS generation and mitochondria-mediated caspase-dependent apoptotic events (40). We found TRAP1 modulates apoptosis via controlling ROS accumulation. Silencing TRAP1 expression increases intracellular ROS accumulation, whereas TRAP1 overexpression reduces ROS production. This suggests TRAP1 may play an important role in regulation of oxidative stress of the cell.

Acknowledgments—We thank Drs. D. O. Toft, S. J. Felts, and Guifang Chen for their reagents and Chunchun Liu, Youli Xu, Lei Sun, and Yan Teng for their technical help.

REFERENCES

1. Trapani, J. A., and Smyth, M. J. (2002) *Nat. Rev. Immunol.* **2,** 735–747
2. Fan, Z., and Zhang, Q. (2005) *Cell Mol. Immunol.* **2,** 259–264
3. Russell, J. H., and Ley, T. J. (2002) *Annu. Rev. Immunol.* **20,** 323–370
4. Fan, Z., Beresford, P. J., Oh, D. Y., Zhang, D., and Lieberman, J. (2003) *Cell* **112,** 659–672
5. Fan, Z., Beresford, P. J., Zhang, D., and Lieberman, J. (2002) *Mol. Cell Biol.* **22,** 2810–2820
6. Lieberman, J., and Fan, Z. (2003) *Curr. Opin. Immunol.* **15,** 553–559
7. Fan, Z., Beresford, P. J., Zhang, D., Xu, Z., Novina, C. D., Yoshida, A., Pommier, Y., and Lieberman, J. (2003) *Nat. Immunol.* **4,** 145–153
8. Bots, M., and Medema, J. P. (2006) *J. Cell Science* **119,** 5011–5014
9. Grossman, W. J., Revell, P. A., Lu, Z. H., Johnson, H., Bredemeyer, A. J., and Ley, T. J. (2003) *Curr. Opin. Immunol.* **15,** 544–552
10. Smyth, M. J., Wiltrout, T., Trapani, J. A., Ottaway, K. S., Sowder, R., Henderson, L. E., Kam, C. M., Powers, J. C., Young, H. A., and Sayers, T. J. (1992) *J. Biol. Chem.* **267,** 24418–24425
11. Sayers, T. J., Brooks, A. D., Ward, J. M., Hoshino, T., Bere, W. E., Wiegand, G. W., Kelly, J. M., and Smyth, M. J. (2001) *J. Immunol.* **166,** 765–771
12. Kelly, J. M., Waterhouse, N. J., Cretney, E., Browne, K. A., Ellis, S., Trapani, J. A., and Smyth, M. J. (2004) *J. Biol. Chem.* **279,** 22236–22242
13. Lu, H., Hou, Q., Zhao, T., Zhang, H., Zhang, Q., Wu, L., and Fan, Z. (2006) *J. Immunol.* **177,** 1171–1178
14. Danial, N. N., and Korsmeyer, S. J. (2004) *Cell* **116,** 205–219
15. Alimonti, J. B., Shi, L., Baijal, P. K., and Greenberg, A. H. (2001) *J. Biol. Chem.* **276,** 6974–6982
16. Heibein, J. A., Goping, I. S., Barry, M., Pinkoski, M. J., Shore, G. C., Green, D. R., and Bleackley, R. C. (2000) *J. Exp. Med.* **192,** 1391–1402
17. Barry, M., Heibein, J. A., Pinkoski, M. J., Lee, S. F., Moyer, R. W., Green, D. R., and Bleackley, R. C. (2000) *Mol. Cell Biol.* **20,** 3781–3794
18. Heibein, J. A., Barry, M., Motyka, B., and Bleackley, R. C. (1999) *J. Immunol.* **163,** 4683–4693
19. Johnson, H., Scorrano, L., Korsmeyer, S. J., and Ley, T. J. (2003) *Blood* **101,** 3093–3101
20. MacDonald, G., Shi, L., Vande Velde, C., Lieberman, J., and Greenberg, A. H. (1999) *J. Exp. Med.* **189,** 131–144
21. Martinvalet, D., Zhu, P., and Lieberman, J. (2005) *Immunity* **22,** 355–370
22. Song, H. Y., Dunbar, J. D., Zhang, Y. X., Guo, D., and Donner, D. B. (1995) *J. Biol. Chem.* **270,** 3574–3581
23. Chen, C. F., Chen, Y., Dai, K., Chen, P. L., Riley, D. J., and Lee, W. H. (1996) *Mol. Cell Biol.* **16,** 4691–4699
24. Felts, S. J., Owen, B. A., Nguyen, P., Trepel, J., Donner, D. B., and Toft, D. O. (2000) *J. Biol. Chem.* **275,** 3305–3312
25. Masuda, Y., Shima, G., Aiuchi, T., Horie, M., Hori, K., Nakajo, S., Kajimoto, S., Shibayama-Imazu, T., and Nakaya, K. (2004) *J. Biol. Chem.* **279,** 42503–42515
26. Im, C. N., Lee, J. S., Zheng, Y., and Seo, J. S. (2007) *J. Cell. Biochem.* **100,** 474–486
27. Zhao, T., Zhang, H., Guo, Y., and Fan, Z. (2007) *J. Biol. Chem.* **282,** 12104–12111
28. Kempaiah, R. K., and Srinivasan, K. (2006) *J. Nutr. Biochem.* **17,** 471–478
29. Waterhouse, N. J., Sedelies, K. A., Sutton, V. R., Pinkoski, M. J., Thia, K. Y., Johnstone, R., Bird, P. I., Green, D. R., and Trapani, J. A. (2006) *Cell Death Differ.* **13,** 607–618
30. Brummelkamp, T. R., Bernards, R., and Agami, R. (2002) *Science* **296,** 550–553
31. Voisine, C., Craig, E. A., Zufall, N., von Ahsen, O., Pfanner, N., and Voos, W. (1999) *Cell* **97,** 565–574
32. Ricci, J. E., Gottlieb, R. A., and Green, D. R. (2003) *J. Cell Biol.* **160,** 65–75
33. Esposito, L. A., Melov, S., Panov, A., Cottrell, B. A., and Wallace, D. C. (1999) *Proc. Natl. Acad. Sci. U. S. A.* **96,** 4820–4825
34. Pandey, P., Saleh, A., Nakazawa, A., Kumar, S., Srinivasula, S. M., Kumar, V., Weichselbaum, R., Nalin, C., Alnemri, E. S., Kufe, D., and Kharbanda, S. (2000) *EMBO J.* **19,** 4310–4322
35. Kluck, R. M., Bossy-Wetzel, E., Green, D. R., and Newmeyer, D. D. (1997) *Science* **275,** 1132–1136
36. Li, P., Nijhawan, D., Budihardjo, I., Srinivasula, S. M., Ahmad, M., Alnemri, E. S., and Wang, X. (1997) *Cell* **91,** 479–489
37. Fan, Z., Yu, P., Wang, Y., Wang, Y., Fu, M. L., Liu, W., Sun, Y., and Fu, Y. X. (2006) *Blood* **107,** 1342–1351
38. Suck, G., Branch, D. R., Smyth, M. J., Miller, R. G., Vergidis, J., Fahim, S., and Keating, A. (2005) *Exp. Hematol.* **33,** 1160–1171
39. Jiang, X., and Wang, X. (2004) *Annu. Rev. Biochem.* **73,** 87–106
40. Lee, Y. J., Lee, D. H., Cho, C. K., Chung, H. Y., Bae, S., Jhon, G. J., Soh, J. W., Jeoung, D. I., Lee, S. J., and Lee, Y. S. (2005) *Oncogene* **24,** 3715–3725